0022-3565/04/3103-1035–1045$20.00
THE JOURNAL OF PHARMACOLOGY AND EXPERIMENTAL THERAPEUTICS
JPET 310:1035–1045, 2004

Vol. 310, No. 3
68098/1163343
Printed in U.S.A.

Lobeline Analogs with Enhanced Affinity and Selectivity for Plasmalemma and Vesicular Monoamine Transporters

Dennis K. Miller,[1] Peter A. Crooks, Guangrong Zheng, Vladimir P. Grinevich,[2] Seth D. Norrholm,[3] and Linda P. Dwoskin

College of Pharmacy, University of Kentucky, Lexington, Kentucky

Received March 9, 2004; accepted April 28, 2004

ABSTRACT

Lobeline attenuates the behavioral effects of psychostimulants in rodents and inhibits the function of nicotinic receptors (nAChRs), dopamine transporters (DATs), and vesicular monoamine transporters (VMAT2s). Monoamine transporters are considered valid targets for drug development for the treatment of methamphetamine abuse. In the current study, a series of lobeline analogs were evaluated for affinity and selectivity at these targets. None of the analogs was more potent than nicotine at the [^{3}H]methyllycaconitine binding site ($\alpha7*$ nAChR subtype). Lobeline tosylate was equipotent with lobeline in inhibiting [^{3}H]nicotine binding but 70-fold more potent in inhibiting nicotine-evoked $^{86}Rb^+$ efflux, demonstrating antagonism of $\alpha4\beta2*$ nAChRs. Compared with lobeline, the defunctionalized analogs lobelane, mesotransdiene, and (−)-*trans*-transdiene showed dramatically reduced affinity at $\alpha4\beta2*$ nAChRs and a 15- to 100-fold higher affinity (K_i = 1.95, 0.58, and 0.26 μM, respectively) at DATs. Mesotransdiene and (−)-*trans*-transdiene competitively inhibited DAT function, whereas lobelane and lobeline acted noncompetitively. 10*S*/10*R*-MEPP [*N*-methyl-2*R*-(2*R*/2*S*-hydroxy-2-phenylethyl)6*S*-(2-phenylethyl)piperidine] and 10*R*-MESP [*N*-methyl-2*R*-(2*R*-hydroxy-2-phenylethyl)6*S*-(2-phenylethen-1-yl)piperidine] were 2 to 3 orders of magnitude more potent (K_i = 0.01 and 0.04 μM, respectively) than lobeline in inhibiting [^{3}H]serotonin uptake; 10*S*/10*R*-MEPP showed a 600-fold selectivity for this transporter. Uptake results using hDATs and human serotonin transporters expressed in human embryonic kidney-293 cells were consistent with native transporter assays. Lobelane and ketoalkene were 5-fold more potent (K_i = 0.92 and 1.35 μM, respectively) than lobeline (K_i = 5.46 μM) in inhibiting [^{3}H]methoxytetrabenazine binding to VMAT2 in vesicle preparations. Thus, structural modification (defunctionalization) of the lobeline molecule markedly decreases affinity for $\alpha4\beta2*$ and $\alpha7*$ nAChRs while increasing affinity for neurotransmitter transporters, affording analogs with enhanced selectivity for these transporters and providing new leads for the treatment of psychostimulant abuse.

Lobeline, an alkaloid from Indian tobacco, inhibits the behavioral and neurochemical effects of psychostimulant drugs of abuse. For example, lobeline attenuates *d*-amphetamine-, methamphetamine- and nicotine-induced hyperactivity (Green et al., 2001; Miller et al., 2001, 2002) and inhibits the discriminative stimulus effects of methamphetamine (Miller et al., 2001). Although lobeline is not self-administered, it decreases methamphetamine self-administration in rats, which is not surmounted by increasing methamphetamine unit doses (Harrod et al., 2001, 2003). These results suggest that lobeline lacks abuse liability while decreasing the stimulant and rewarding effects of methamphetamine via a noncompetitive mechanism of action.

Psychostimulant-induced behavioral activation and reinforcement are at least partly mediated via interaction with neurotransmitter transporters that regulate synaptic dopamine (DA) concentrations (Wise and Bozarth, 1987; Koob, 1992). Methamphetamine is a substrate for the DA trans-

This research was supported by NIH Grants DA 06043, DA 07304, DA 00399, and DA 13519. National Institute on Drug Abuse Interagency Agreement Y1DA-0107 supported the studies assessing the interaction of lobeline, lobelane, and MTD at the human neurotransmitter transporters expressed in HEK-293 cells. For purposes of full disclosure, the University of Kentucky holds patents on lobeline, which have been licensed by Yaupon Therapeutics, Inc. (Lexington, KY). A potential royalty stream to L.P.D. and P.A.C. may occur consistent with University of Kentucky policy, and both L.P.D. and P.A.C. are founders of, and have financial interest in, Yaupon Therapeutics, Inc.

[1] Current address: Department of Psychological Sciences, University of Missouri, Columbia, MO 65211.

[2] Current address: Targacept, Inc., 200 East First Street, Suite 300, Winston-Salem, NC 27101-4165.

[3] Current address: Department of Anatomy, College of Medicine, University of South Florida, 12901 Bruce B. Downs Blvd., MDC 6, Tampa, FL 33612-4799.

Article, publication date, and citation information can be found at http://jpet.aspetjournals.org.
doi:10.1124/jpet.104.068098.

ABBREVIATIONS: DA, dopamine; DAT, DA transporter; VMAT2, vesicular monoamine transporter; SERT, serotonin transporter; nAChR, nicotinic receptor; 5-HT, serotonin; NE, norepinephrine; NET, NE transporter; MLA, methyllycaconitine; RTI-55, (−)-2β-carbomethoxy-3β-(4-iodophenyl)tropane; MTBZ, methoxytetrabenazine; BSA, bovine serum albumin; PEI, phenylethylenimine; TTX, tetrodotoxin; 10*R*-MESP, *N*-methyl-2*R*-(2*R*-hydroxy-2-phenylethyl)6*S*-(2-phenylethen-1-yl)piperidine; 10*S*/10*R*-MEPP, *N*-methyl-2*R*-(2*R*/2*S*-hydroxy-2-phenylethyl)6*S*-(2-phenylethyl)piperidine; MTD, mesotransdiene; TTD, *trans*-transdiene; GBR-12909, 1-(2-[bis(4-fluorophenyl)methoxy]ethyl)4-(3-phenylpropyl)piperazine; HEK, human embryonic kidney; SAR, structure-activity relationship.

porter (DAT) (Sulzer et al., 1995; Johnson et al., 1998) and decreases the activity of the vesicular monoamine transporter (VMAT2) (Brown et al., 2000, 2001). Studies with VMAT2 knockout mice in which amphetamine-induced conditioned place preference is attenuated (Takahashi et al., 1997) support a role for VMAT2 in mediating the behavioral effects of stimulant drugs. Although effects on DAT, SERT, and/or VMAT2 may not be the only mechanisms responsible for the reinforcing properties of psychostimulants (Rocha et al., 1998; Sora et al., 1998), these neurotransmitter transporters are considered prime targets for developing pharmacotherapies to treat psychostimulant abuse.

Until recently, the pharmacological activity of lobeline was believed to primarily result from its high-affinity (K_i = 4-20 nM) interaction with nicotinic acetylcholine receptors (nAChRs) (Abood et al., 1988; Reavill et al., 1990; Bhat et al., 1991; Court et al., 1994). Lobeline inhibits nAChR subtypes mediating both nicotine-evoked [^{3}H]DA release and nicotine-evoked $^{86}Rb^+$ efflux (Miller et al., 2000); however, lobeline also interacts with VMAT2 and DAT (Dwoskin and Crooks, 2002). Lobeline potently inhibits [^{3}H]dihydroxytetrabenazine binding to VMAT2 (IC_{50} = 0.90 μM) and inhibits [^{3}H]DA uptake (IC_{50} = 0.88 μM) into rat striatal vesicle preparations (Teng et al., 1997, 1998) and is furthermore ~90-fold less potent (IC_{50} = 80 μM) in inhibiting [^{3}H]DA uptake into rat striatal synaptosomes (Teng et al., 1997). In addition to inhibiting DAT and VMAT2 function, high concentrations of lobeline (10–50 μM) increase [^{3}H]serotonin (5-HT) release from rat hippocampal slices in a mecamylamine-insensitive manner (Lendvai et al., 1996), suggesting that lobeline interacts with SERT. Thus, in addition to interacting with nAChRs, lobeline inhibits VMAT2 more potently than DAT or SERT, suggesting that VMAT2 may be a critical target for its pharmacological activity.

Consistent with the observation that lobeline is not self-administered in rats (Harrod et al., 2003), lobeline does not evoke DA release but stimulates dihydroxyphenylacetic acid overflow (Teng et al., 1997), which likely results from alterations in presynaptic DA storage via an interaction of lobeline with VMAT2 (Dwoskin and Crooks, 2002). Furthermore, lobeline inhibits *d*-amphetamine- and methamphetamine-evoked DA release from superfused rat striatal slices (Miller et al., 2001; S. Krishnamurthy, G. Zheng, P. A. Crooks, and L. P. Dwoskin, manuscript submitted for publication). These results are consistent with the effect of lobeline in inhibiting methamphetamine self-administration (Harrod et al., 2001). These preclinical data suggest that lobeline has potential as a pharmacotherapy for psychostimulant abuse.

Structural modification of the lobeline molecule has afforded compounds with differing affinities for nAChRs (Flammia et al., 1999); however, these analogs have not been evaluated for their activity at neurotransmitter transporters. The present study evaluates a series of lobeline analogs for their activities at $\alpha4\beta2*$ nAChRs, $\alpha7*$ nAChRs, DAT, SERT, NET, and VMAT2 with the aim of identifying analogs with high affinity and selectivity for these target sites. The exact subunit composition, stoichiometry, and arrangement of native nAChRs remain to be elucidated, which is indicated by an asterisk (*) following the subunit designation (Lukas et al., 1999). Such analogs may be useful candidates for probing specific targets for elucidating the underlying neurochemical mechanism(s) responsible for lobeline-induced inhibition of the behavioral effects of methamphetamine.

Materials and Methods

Animals. Male Sprague-Dawley rats (200–250 g upon arrival) were purchased from Harlan (Indianapolis, IN) and housed two per cage with ad libitum access to food and water in the Division of Laboratory Animal Resources at the College of Pharmacy at the University of Kentucky (Lexington, KY). Experimental protocols involving the animals were in accordance with the *NIH Guide for the Care and Use of Laboratory Animals* and were approved by the Institutional Animal Care and Use Committee at the University of Kentucky.

Chemicals. [^{3}H]DA (specific activity, 25.6 Ci/mmol); (±)-[^{3}H]methyllycaconitine (MLA; specific activity, 25.4 Ci/mmol); *S*(−)-[^{3}H]nicotine (specific activity, 80 Ci/mmol); [^{3}H]norepinephrine (NE; specific activity 27.5 Ci/mmol); ^{86}RbCl (specific activity, 55.2 mCi/mmol); [^{125}I]RTI-55 (specific activity, 2200 Ci/mmol); and [^{3}H]serotonin (5-HT; specific activity, 27.5 Ci/mmol) were purchased from PerkinElmer Life and Analytical Sciences (Boston, MA). [^{3}H]MTBZ (specific activity, 56.8 Ci/mmol) was a generous gift from Dr. Michael Kilbourn (Department of Radiology, University of Michigan Medical School, Ann Arbor, MI). Bovine serum albumin (BSA), catechol, dopamine, EDTA, EGTA, fluoxetine HCl, GBR-12909 HCl, HEPES, *S*(−)-nicotine ditartrate (nicotine), nomifensine maleate, pargyline HCl, polyethylenimine (PEI), serotonin, tetrodotoxin (TTX), tris[hydroxymethyl]aminomethane hydrochloride (Trizma HCl), tris[hydroxymethyl]-aminomethane base (Trizma), and tropolone were purchased from Sigma-Aldrich (St. Louis, MO). α-D-Glucose, L-ascorbic acid, and potassium phosphate monobasic were purchased from Aldrich Chemical Co. (Milwaukee, WI), AnalaR-BHD Ltd. (Poole, UK), and Mallinckrodt (St. Louis, MO), respectively. Lobeline hemisulfate was purchased from MP Biomedicals (Irvine, CA). All other commercially obtained chemicals were purchased from Fisher Scientific Co. (Pittsburgh, PA).

The lobeline analogs ketoalkene (*N*-methyl-2*R*-(2-oxo-2-phenylethyl)6*S*-(2-phenylethen-1-yl)piperidine), 10*R*-MESP, 10*S*/10*R*-MEPP, lobelanidine, lobelanine, mesotransdiene (MTD), (−)-*trans*-transdiene (TTD), lobelane, and lobeline tosylate (lobeline-8-*O*-tosylate) were synthesized by structural modification of the lobeline molecule (G. Zheng, L. P. Dwoskin, A. G. Deaciuc, and P. A. Crooks, manuscript submitted for publication) and are illustrated in Fig. 1. The structures of the lobeline analogs were verified by ^{1}H and ^{13}C NMR spectroscopy, mass spectrometry, and, in some cases, X-ray crystallography.

[^{3}H]Nicotine Binding Assay. Striata from 2 to 4 rats were homogenized using a Tekmar polytron (Tekmar-Dohrmann, Mason, OH) in 10 volumes of ice-cold modified Krebs-HEPES buffer (20 mM HEPES, 118 mM NaCl, 4.8 mM KCl, 2.5 mM $CaCl_2$, and 1.2 mM $MgSO_4$, pH 7.5). Homogenates were incubated (5 min at 37°C) and centrifuged (29,000*g* for 20 min at 4°C). Resulting pellets were resuspended in 10 volumes of ice-cold MilliQ water (Millipore Corporation, Molsheim, France), incubated (5 min at 37°C), and centrifuged (29,000*g* for 20 min at 4°C). Resulting pellets were again resuspended in 10 volumes of ice-cold 10% Krebs-HEPES buffer and then incubated and centrifuged as described above. Final pellets were stored at −70°C in fresh 10% Krebs-HEPES buffer until use. Upon assay, pellets were resuspended in 10% Krebs-HEPES buffer, incubated, and centrifuged as described above. Final pellets were resuspended in ice-cold MilliQ water (2.0 ml) to provide ~200 μg of protein/100 μl of membrane suspension. Inhibition of specific [^{3}H]nicotine binding by lobeline and its analogs was assessed using a previously described method (Crooks et al., 1995). Briefly, assays were performed in triplicate in a final volume of 200 μl of Krebs-HEPES buffer containing 250 mM Tris (pH 7.5, 4°C). Reactions were initiated by the addition of 100 μl of membrane suspension to tubes containing 50 μl of Krebs-HEPES buffer or 1 of 9 concentrations (final concentration, 0.1 nM–1 mM) of nicotine, lobeline, or analog

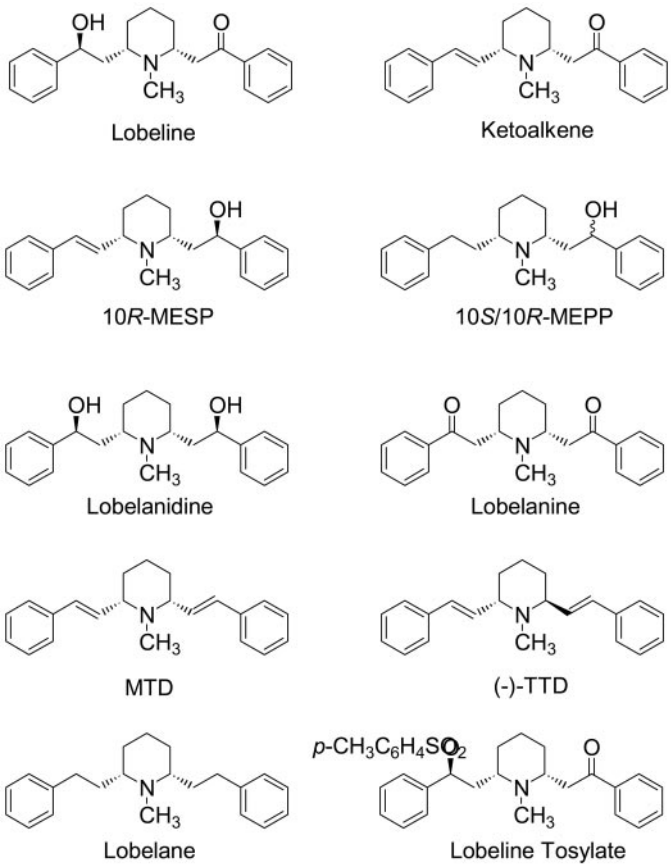

Fig. 1. Chemical structures of lobeline and lobeline analogs.

and 50 μl of [^{3}H]nicotine (final concentration, 3 nM). Nonspecific binding was determined in triplicate in the presence of nicotine (10 μM). Following incubation (90 min at 4°C), reactions were terminated by the dilution of samples with ice-cold Krebs-HEPES buffer followed by immediate filtration through Whatman GF/B glass fiber filters (presoaked in 0.5% PEI) using a cell harvester (MP-43RS; Brandel Inc., Gaithersburg, MD). Filters were processed, and radioactivity was determined by liquid scintillation spectroscopy (B1600TR scintillation counter; PerkinElmer Life and Analytical Sciences).

[^{3}H]MLA Binding Assay. Whole rat brain (minus cortex, striatum, and cerebellum) was homogenized in 20 volumes of ice-cold hypotonic buffer (2 mM HEPES, 14.4 mM NaCl, 0.15 mM KCl, 0.2 mM $CaCl_2$, and 0.1 mM $MgSO_4$, pH 7.5). Homogenates were incubated at 37°C for 10 min and centrifuged (25,000*g* for 15 min at 4°C). Pellets were washed three times by resuspension in 20 volumes of buffer and followed by centrifugation. Final pellets were resuspended in the incubation buffer to provide ~150 μg of protein/100 μl of membrane suspension. Binding assays were performed in duplicate in a final volume of 250 μl of incubation buffer containing 20 mM HEPES, 144 mM NaCl, 1.5 mM KCl, 2 mM $CaCl_2$, 1 mM $MgSO_4$, and 0.05% BSA, pH 7.5. Assays were initiated by the addition of 100 μl of membrane suspension to 150 μl of sample containing 2.5 nM [^{3}H]MLA and 1 of 8 concentrations (final concentration, 30 nM–100 μM) of lobeline or analog and incubated for 2 h at room temperature. Nonspecific binding was determined in the presence of nicotine (1 mM). Assays were terminated by dilution with ice-cold incubation buffer (3 ml) followed by immediate filtration through glass fiber filters (Schleicher and Schuell, Inc., Keene, NH) presoaked with 0.5% PEI using a cell harvester (MP-43RS; Brandel Inc.). Filters were processed, and radioactivity was determined as described above.

$^{86}Rb^+$ Efflux Assay. The ability of lobeline and its analogs to evoke $^{86}Rb^+$ efflux was determined using a previously published method (Miller et al., 2000). nAChR-mediated $^{86}Rb^+$ efflux from preloaded rodent brain synaptosomes has been used to characterize functional interactions of ligands with [^{3}H]nicotine binding sites based on the findings that the response to nAChR agonists in the $^{86}Rb^+$ efflux assay is highly correlated with the displacement of high-affinity [^{3}H]nicotine binding ($\alpha4\beta2*$ nAChRs) and nAChR agonist-evoked $^{86}Rb^+$ efflux is eliminated when brain from $\beta2$-subunit knockout mice is used (Marks et al., 1993, 1995, 1999; Sharples et al., 2000). In the current study, thalamus was homogenized and centrifuged (1000*g* for 10 min at 4°C). Supernatants were centrifuged (12,000*g* for 20 min at 4°C) to obtain synaptosomes. Synaptosomes were incubated for 30 min in 35 μl of uptake buffer (140 mM NaCl, 1.5 mM KCl, 2.0 mM $CaCl_2$, 1.0 mM $MgSO_4$, and 20 mM α-D-glucose, pH 7.5) containing $^{86}Rb^+$ (4 μCi). $^{86}Rb^+$ uptake was terminated by filtration onto glass fiber filters (6 mm, type A/E; Gelman Instrument Co., Ann Arbor, MI) under gentle vacuum (0.2 atm) and followed by three washes with uptake buffer (0.5 ml each). Each filter with $^{86}Rb^+$-loaded synaptosomes (~40 μg of protein/μl) was subsequently placed on a glass fiber filter (13 mm, type A/E) mounted on a polypropylene platform. Synaptosomes were superfused at a rate of 2.5 ml/min with $^{86}Rb^+$ efflux assay buffer (125 mM NaCl, 5 mM CsCl, 1.5 mM KCl, 2 mM $CaCl_2$, 1 mM $MgSO_4$, 25 mM HEPES, 20 mM α-D-glucose, 0.1 μM TTX, and 1.0 g/l BSA, pH 7.5). TTX and CsCl were included in the buffer to block voltage-gated Na^+ and K^+ channels, respectively, and to reduce the rate of basal $^{86}Rb^+$ efflux. Lobeline- and analog-induced $^{86}Rb^+$ efflux (intrinsic activity) and lobeline- and analog-induced inhibition of nicotine-evoked $^{86}Rb^+$ efflux were determined. For these assays, the concentration (1 μM) of nicotine was chosen based on previous observations that this was the lowest concentration producing maximal $^{86}Rb^+$ efflux (~1.0% tissue content) (Miller et al., 2000). After 8 min of superfusion, basal samples were collected for 2 min. Synaptosomes were subsequently superfused for 3 min with 1 of 5 concentrations (1 nM–100 μM) of lobeline or analog. Nicotine was then added to the buffer containing lobeline or analog, and superfusion continued for 3 min. Each aliquot part of thalamic synaptosomes was exposed to only one concentration of lobeline or analog. In each experiment, one synaptosomal aliquot part was also exposed to nicotine in the absence of lobeline or analog, and one synaptosomal aliquot part was superfused in the absence of lobeline, analog, and nicotine to determine basal $^{86}Rb^+$ efflux during the entire course of the experiment. Samples were analyzed using liquid scintillation spectroscopy as described above.

Inhibition of [^{3}H]DA and [^{3}H]5-HT Uptake into Rat Striatal and Hippocampal Synaptosomes, Respectively. Lobeline- and analog-induced inhibition of [^{3}H]DA and [^{3}H]5-HT uptake into rat striatal and hippocampal synaptosomes, respectively, was assessed using modifications of a previously described method (Teng et al., 1997). Analog-induced inhibition was compared with that induced by the selective DAT and SERT transporter inhibitors GBR-12909 and fluoxetine, respectively (Fuller et al., 1991; Carroll et al., 2002). Brain regions were homogenized in 20 ml of ice-cold 0.32 M sucrose solution containing 5 mM $NaHCO_3$ (pH 7.4) with 12 up-and-down strokes of a Teflon pestle homogenizer (clearance ≈ 0.003). Homogenates and supernatants were centrifuged at 2,000*g* for 10 min at 4°C and 20,000*g* for 15 min at 4°C, respectively. Pellets were resuspended in 1.5 ml of Krebs buffer (125 mM NaCl, 5 mM KCl, 1.5 mM $MgSO_4$, 1.25 mM $CaCl_2$, 1.5 mM KH_2PO_4, 10 mM α-D-glucose, 25 mM HEPES, 0.1 mM EDTA, 0.1 mM pargyline, and 0.1 mM ascorbic acid saturated with 95% O_2/5% CO_2, pH 7.4). Final protein concentrations were 400 μg/ml and were determined by protein-dye binding (Bradford, 1976). Assays were performed in duplicate in a total volume of 500 μl. Aliquot parts of synaptosomal suspension (50 μl) were added to tubes containing 350 μl of Krebs buffer and 50 μl of buffer containing final concentrations of 1 nM to 1 mM lobeline, lobeline analog, GBR-12909, fluoxetine, or 50 μl of buffer without drug. Tubes were incubated at 34°C for 10 min before the addition of

50 μl of [3H]DA (final concentration, 10 nM) or 50 μl of [3H]5-HT (final concentration, 10 nM). Accumulation proceeded for 10 min at 34°C. Reactions were terminated by the addition of 3 ml of ice-cold Krebs buffer. Nonspecific [3H]DA and [3H]5-HT uptake was determined in the presence of nomifensine (10 μM) and fluoxetine (10 μM), respectively. Samples were rapidly filtered through a Whatman GF/B filter using a cell harvester (MP-43RS; Brandel Inc.), and filters were subsequently washed three times with 4 ml of ice-cold Krebs buffer containing catechol (1 mM). Radioactivity retained by the filters was determined by liquid scintillation spectroscopy (B1600 TR scintillation counter; PerkinElmer Life and Analytical Sciences).

Kinetic Analysis of [3H]DA Uptake into Rat Striatal Synaptosomes. To determine whether the inhibition of [3H]DA uptake was via a competitive or noncompetitive mechanism, kinetic analyses were performed for lobeline (60 μM), MTD (3 μM), (−)-TTD (1 μM), and lobelane (1 μM). The concentrations used in the kinetic analyses were chosen to approximate the IC_{50} values from the above concentration-response experiments for analog-induced inhibition of [3H]DA uptake. Experiments were conducted in the absence and presence of lobeline or analog. The absence of lobeline or analog (buffer alone) represented the control condition. Nonspecific uptake was determined in the presence of nomifensine (10 μM). In the absence and presence of nomifensine, aliquot parts of rat striatal synaptosomal suspension (50 μl) were added to tubes containing 350 μl of Krebs buffer and 50 μl of lobeline, analog, or buffer alone. Tubes were incubated for 5 min at 34°C. Uptake was initiated by the addition of [3H]DA [final concentration, 1 nM–5 μM, 50 μl, isotopically diluted with unlabeled DA (0.3–83 μM) to achieve varying DA concentrations and a consistent amount of radioactivity (i.e., 500,000 dpm per tube)]. Accumulation proceeded for 10 min at 34°C. Reactions were terminated by the addition of 3 ml of ice-cold Krebs buffer. Samples were washed three times with 4 ml of ice-cold Krebs buffer containing catechol (1 mM) and filtered. Radioactivity retained by the filters was determined by liquid scintillation spectroscopy as described above.

Inhibition of [125I]RTI-55 Binding to hDAT, hSERT, and hNET Stably Expressed in HEK-293 cells. Lobeline-, lobelane- and MTD-induced inhibition of [125I]RTI-55 binding to hDAT, hSERT, and hNET was assessed using a previously described method (Eshleman et al., 1999). HEK-hDAT and HEK-hSERT cells were incubated in Dulbecco's modified Eagle's medium supplemented with 5% fetal bovine serum, 5% calf bovine serum, 0.05 U of penicillin/streptomycin, and puromycin (2 μg/ml). HEK-hNET cells were incubated in Dulbecco's modified Eagle's medium supplemented with 10% fetal bovine serum, 0.05 U of penicillin/streptomycin, and geneticin (300 μg/ml). HEK-293 cells stably expressing hDAT, hSERT, or hNET were grown to 80% confluence on 150-mm diameter tissue culture dishes in a humidified 10% CO_2 environment at 37°C. The medium was poured off the plates, and the plates were washed with 10 ml of calcium- and magnesium-free phosphate-buffered saline. Lysis buffer (2 mM HEPES with 1 mM EDTA) was added, and the plates were placed on ice. After 10 min, cells were scraped from the plates and centrifuged (30,000*g* for 20 min). Pellets were resuspended in 12 to 32 ml of 0.32 M sucrose using a Polytron homogenizer (setting 7 for 10 s). Resuspension volumes depended on the density of binding sites within a cell line, providing binding of <10% of the total radioactivity. Analog-induced inhibition of [125I]RTI-55 binding was compared with that induced by cocaine as the standard. Nonspecific binding was determined in the presence of mazindol (5 μM) for hDAT and hNET assays or imipramine (5 μM) for the hSERT assays. Competition assays were conducted with duplicate determinations for each point. Aliquot parts of membranes (50 μl, ~10–15 μg of protein) were added to tubes containing 15 μl of inhibitor (lobeline, lobelane, MTD, or cocaine; 20 nM–10 μM) or Krebs-HEPES assay buffer (122 mM NaCl, 2.5 mM $CaCl_2$, 1.2 mM $MgSO_4$, 10 μM pargyline, 100 μM tropolone, 0.2% glucose, and 0.02% ascorbic acid buffered with 25 mM HEPES, pH 7.4). Tubes containing membranes and inhibitor were preincubated at room temperature for 10 min before the addition of 25 μl of [125I]RTI-55 (final concentration, 40–80 pM) and sufficient Krebs-HEPES buffer to obtain a final volume of 250 μl. Tubes were incubated at 25°C for 90 min. Binding was terminated by filtration over GF/C filters using a 96-well cell harvester. Filters were washed for 6 s with ice-cold saline. Scintillation fluid (50 μl) was added to each tube, and radioactivity remaining on the filter was determined using a Wallac MicroBeta or Betaplate scintillation counter (EG & G Wallac, Turku, Finland).

Inhibition of [3H]DA, [3H]5-HT, and [3H]NE Uptake by hDAT, hSERT, and hNET, Respectively, in Stably Expressed HEK-293 Cells. Lobeline-, lobelane- and MTD-induced inhibition of [3H]DA, [3H]5-HT, and [3H]NE uptake by hDAT, hSERT, or hNET, respectively, in HEK-293 cells stably expressing these transporters was assessed using a previously described method (Eshleman et al., 1999). HEK-hDAT, HEK-hSERT, and HEK-hNET were grown on 150-mm diameter culture dishes as described above. The medium was removed, and cells were washed twice with phosphate-buffered saline at room temperature. Following the addition of 3 ml of Krebs-HEPES buffer, plates were placed in a 25°C water bath for 5 min. The cells were gently scraped, and clusters were separated by trituration using a pipette for 5 to 10 aspirations and ejections. Cells from multiple plates were combined for use in assays. Analog-induced inhibition was compared with that induced by cocaine as the standard. Nonspecific uptake was determined in the presence of mazindol (5 μM) for hDAT and hNET assays or imipramine (5 μM) for hSERT assays. Aliquot parts of cell preparation (50 μl) were added to 1-ml vials containing 350 μl of Krebs-HEPES buffer, 50 μl of inhibitor (lobeline, lobelane, MTD, or cocaine; 20 nM–10 μM), and 50 μl of either mazindol or imipramine in a final assay volume of 500 μl to determine nonspecific uptake. Tubes were incubated at 25°C for 10 min before the addition of 50 μl of [3H]DA, [3H]5-HT, or [3H]NE (final concentration, 20 nM). Accumulation of [3H]neurotransmitter proceeded for 10 min. Reactions were terminated by filtration through Whatman GF/C filters presoaked in 0.05% polyethylenimine. Scintillation cocktail was added, and radioactivity remaining on the filter was determined as described above for the binding assay.

Inhibition of [3H]MTBZ Binding to Vesicles Prepared from Rat Whole Brain. Lobeline- and analog-induced inhibition of [3H]MTBZ binding was determined using modifications of a previously described method for [3H]dihydroxytetrabenazine binding (Teng et al., 1998). Nonspecific binding was determined in the presence of tetrabenazine (20 μM). Rat whole brain (excluding cerebellum) was homogenized in 20 ml of ice-cold 0.32 M sucrose solution with seven up-and-down strokes of a Teflon pestle homogenizer (clearance ≈ 0.003). Homogenates and supernatants were centrifuged at 1,000*g* for 12 min at 4°C and 22,000*g* for 10 min at 4°C, respectively. Resulting pellets were incubated in 18 ml of cold water for 5 min, and 2 ml of HEPES (25 mM) and potassium-tartrate (100 mM) solution was subsequently added. Samples were centrifuged (20,000*g* for 20 min at 4°C), and $MgSO_4$ (1 mM) solution was then added to the supernatants. Solutions were centrifuged (100,000*g* for 45 min at 4°C) and resuspended in cold assay buffer (25 mM HEPES, 100 mM potassium-tartrate, 5 mM $MgSO_4$, 0.1 mM EDTA, and 0.05 mM EGTA, pH 7.5). The final protein concentration was 15 μg of protein/100 μl (Bradford, 1976). Assays were performed in duplicate in 96-well plates. Aliquot parts of vesicular suspension (100 μl) were added to wells containing 50 μl of [3H]MTBZ (final concentration, 3 nM), 50 μl of lobeline or analog, and 50 μl of buffer. Reactions were terminated by filtration (Filtermate harvester; PerkinElmer Life and Analytical Sciences) onto Unifilter-96 GF/B filter plates (presoaked in 0.5% polyethylenimine). Filters were subsequently washed five times with 350 μl of ice-cold buffer (25 mM HEPES, 100 mM K_2-tartrate, 5 mM $MgSO_4$, and 10 mM NaCl, pH 7.5). Filter plates were dried and bottom-sealed, and each well was filled with 40 μl of scintillation cocktail (MicroScint 20; PerkinElmer Life and Analytical Sciences). Radioactivity in filters was determined by liquid scintillation

spectroscopy (TopCount NXT scintillation counter; PerkinElmer Life and Analytical Sciences).

Data Analysis. For lobeline- and analog-induced inhibition of [^{3}H]nicotine and [^{3}H]MLA binding, specific binding was determined by subtracting nonspecific binding from total binding. Concentrations of inhibitor that produced 50% inhibition (IC_{50} values) and 95% confidence intervals were determined from the concentration-effect curves via an iterative curve-fitting program (Prism 3.0; GraphPad Software Inc., San Diego, CA). Inhibition constants (K_i values) were determined using the Cheng-Prusoff equation (Cheng and Prusoff, 1973).

For the $^{86}Rb^+$ efflux assay, basal rate of efflux was determined via an exponential decay curve used to fit the data points preceding and following superfusion with lobeline or analog and nicotine (SigmaPlot version 8; Systat Software, Inc., Point Richmond, CA). The lobeline-, analog- or nicotine-evoked increase in $^{86}Rb^+$ efflux was calculated as the fractional increase above baseline. Increases were summed to obtain total $^{86}Rb^+$ efflux during the period of superfusion with lobeline, analog, and/or nicotine and normalized to $^{86}Rb^+$ content in the corresponding synaptosomal sample to reduce variability within and between experiments. To determine intrinsic activity of lobeline or analog, total $^{86}Rb^+$ efflux during the 3-min period of superfusion in the absence of nicotine was analyzed by one-way repeated measures analysis of variance with lobeline or analog concentration as a within-subject factor (SPSS version 9.0; SPSS Inc., Chicago, IL). To assess the lobeline- and analog-induced inhibition of nicotine-evoked $^{86}Rb^+$ efflux, total efflux during the 3-min period of superfusion in the presence of nicotine and lobeline or analog was analyzed by one-way repeated measures analysis of variance with lobeline or analog concentration as a within-subject factor. Concentrations of lobeline or analog that exhibited intrinsic activity were not included in the analysis to determine inhibition of the effect of nicotine. Additionally, IC_{50} values were determined by nonlinear regression fit of the mean data to sigmoidal concentration-response curves (Prism 3.03; GraphPad Software Inc.).

To generate concentration-response curves for the inhibition of [^{3}H]neurotransmitter uptake, specific uptake was determined by subtracting nonspecific uptake from total uptake. Similarly, for the competition binding curves for [^{3}H]MTBZ and [^{125}I]RTI-55, specific binding was determined by subtracting nonspecific from total binding. IC_{50} values were determined from the curves by an iterative curve fitting program (Prism 3.03; GraphPad Software Inc.), and K_i values were calculated using the Cheng-Prusoff equation (Cheng and Prusoff, 1973). For [^{125}I]RTI-55 binding, Hill coefficients were determined. For analysis of [^{3}H]DA uptake kinetics, K_m and V_{max} values were determined from concentration-effect curves for specific [^{3}H]DA uptake (Taylor and Insel, 1990; Kenakin, 1997). Paired two-tailed t tests were performed on the log K_m and V_{max} values to determine differences ($P < 0.05$) between the absence (control condition) and presence of lobeline, MTD, (−)-TTD, or lobelane.

Results

Inhibition of [^{3}H]Nicotine Binding. Figure 2 illustrates the competition curves for lobeline and its analogs to inhibit [^{3}H]nicotine binding to rat striatal membranes and provides the K_i values derived from these competition curves. Lobeline completely inhibited [^{3}H]nicotine binding to rat striatal membranes, and a K_i value of 0.016 μM was obtained. Lobeline was ~3-fold less potent than nicotine in this assay. With the notable exception of MTD, which did not inhibit [^{3}H]nicotine binding, the remaining lobeline analogs inhibited [^{3}H]nicotine binding with wide variation in affinity. The tosyl sulfonic acid ester of lobeline, lobeline tosylate, completely inhibited [^{3}H]nicotine binding and was the most potent (K_i = 0.011 μM) of the lobeline analogs, being equipotent with lobeline. The dehydrated analog ketoalkene and its fully

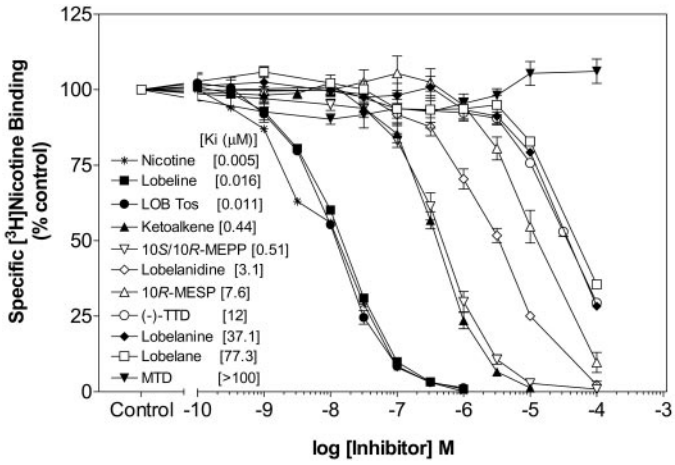

Fig. 2. Lobeline and lobeline analogs inhibit [^{3}H]nicotine binding to rat striatal membranes. Nicotine was used as a standard for comparison. Nonspecific binding was determined in the presence of nicotine (10 μM). K_i values for lobeline and its analogs are provided in brackets. Data are the mean (±S.E.M.) specific binding presented as a percentage of the control condition (mean ± S.E.M., 51.4 ± 2.4 fmol/mg; n = 4 rats per compound).

reduced analog 10*S*/10*R*-MEPP also completely inhibited binding, but these analogs were ~45-fold less potent than lobeline in this assay. The mono and dihydroxy analogs lobelanidine and 10*R*-MESP, respectively, completely inhibited [^{3}H]nicotine binding, and these analogs were more than 2 orders of magnitude less potent than lobeline. The defunctionalized analogs (−)-TTD and lobelane and the diketo analog lobelanine provided ~60% maximal inhibition of [^{3}H]nicotine binding at the concentrations examined, and these analogs were more than 3 orders of magnitude less potent than lobeline. The defunctionalized analog MTD did not inhibit [^{3}H]nicotine binding, demonstrating a lack of interaction of this analog with $\alpha4\beta2*$ nAChRs.

Inhibition of Nicotine-Evoked $^{86}Rb^+$ Efflux. $^{86}Rb^+$ efflux from preloaded rat thalamic synaptosomes has been used as a functional assay for $\alpha4\beta2*$ nAChRs to determine whether compounds act as agonists or antagonists at this site (Marks et al., 1995; Miller et al., 2000). Lobeline has been previously shown to act as a nAChR antagonist in this assay (Miller et al., 2000). Functional effects of the most potent analogs (lobeline tosylate and ketoalkene), as well as the effect of an analog (MTD) that had no affinity for the [^{3}H]nicotine binding site, were assessed in the $^{86}Rb^+$ efflux assay. Neither lobeline nor any of the above analogs evoked $^{86}Rb^+$ efflux (Table 1), demonstrating no agonist activity at $\alpha4\beta2*$ nAChRs. As expected, nicotine (1 μM) evoked an increase in $^{86}Rb^+$ efflux of ~1.0% of total $^{86}Rb^+$ tissue content (Fig. 3). Lobeline inhibited (IC_{50} = 0.73 μM) nicotine-evoked $^{86}Rb^+$ efflux ($F_{6,24}$ = 15.01, $P < 0.001$), consistent with previous results (Miller et al., 2000). Post hoc analysis revealed that 1 and 10 μM lobeline decreased nicotine-evoked $^{86}Rb^+$ efflux compared with control (nicotine alone). Lobeline tosylate, which was equipotent to lobeline in the [^{3}H]nicotine binding assay (Fig. 2), was nearly 70-fold more potent (IC_{50} = 0.011 μM) than lobeline in inhibiting nicotine-evoked $^{86}Rb^+$ efflux ($F_{5,20}$ = 10.76, $P < 0.01$). Post hoc analysis revealed that lobeline tosylate (10 nM–10 μM) inhibited the effect of nicotine. Ketoalkene also inhibited (IC_{50} = 0.30 μM) nicotine-evoked $^{86}Rb^+$ efflux ($F_{5,20}$ = 4.48, $P < 0.05$) and had a similar

TABLE 1

Intrinsic activity of lobeline, lobeline tosylate, ketoalkene, and MTD on $^{86}Rb^+$ efflux from preloaded rat thalamic synaptosomes

Synaptosomes were superfused for a 3-min period in the absence or presence of lobeline or lobeline analog before the addition of nicotine to buffer. Data from the period of superfusion following addition of nicotine to buffer are presented in Fig. 3.

	Lobeline or Lobeline Analog Concentration					
	Control	1 nM	10 nM	100 nM	1 μM	10 μM
Lobeline	0.13 ± 0.04[a]	−0.16 ± 0.22[b]	0.03 ± 0.07	−0.02 ± 0.08	0.44 ± 0.20	0.18 ± 0.08
Lobeline tosylate	0.11 ± 0.06	0.46 ± 0.27	0.14 ± 0.13	0.30 ± 0.32	−0.06 ± 0.06	0.00 ± 0.00
Ketoalkene	0.17 ± 0.14	0.36 ± 0.07	0.16 ± 0.13	0.16 ± 0.10	0.16 ± 0.12	0.01 ± 0.01
MTD	−0.08 ± 0.10	0.03 ± 0.02	0.21 ± 0.03	0.30 ± 0.10	0.31 ± 0.15	0.27 ± 0.11

[a] Data are mean (±S.E.M.) percentages of $^{86}Rb^+$ efflux tissue content.
[b] Negative values indicate that $^{86}Rb^+$ efflux was below that obtained at baseline; $^{86}Rb^+$ efflux induced by a compound was calculated as the fractional change from baseline.

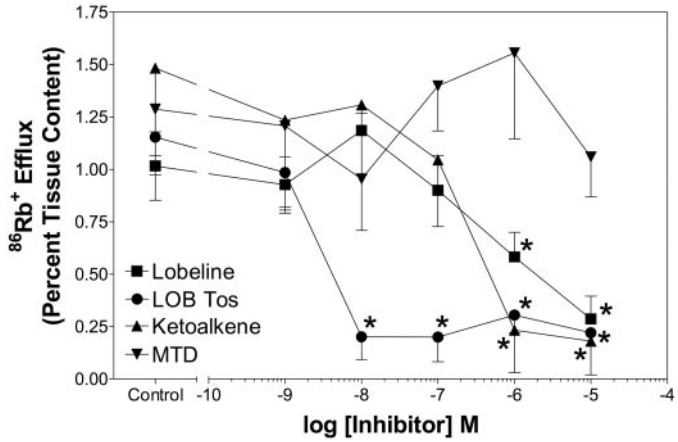

Fig. 3. Lobeline, ketoalkene, and lobeline tosylate, but not MTD, inhibit nicotine (1 μM)-evoked $^{86}Rb^+$ efflux from superfused rat thalamic synaptosomes. Thalamic synaptosomes were superfused with buffer containing lobeline or lobeline analog for 3 min. Nicotine (1 μM) was subsequently added to the buffer, and superfusion continued for an additional 3 min. Data are presented as the mean (±S.E.M.) of the percentage of $^{86}Rb^+$ tissue content during the latter 3-min period of superfusion (n = 5–7 rats per experiment). *, $P < 0.05$ different from control condition.

potency to lobeline in this assay. Post hoc analysis revealed that 1 and 10 μM ketoalkene significantly inhibited the effect of nicotine. In contrast, MTD, which did not interact with the [^{3}H]nicotine binding site (Fig. 2), also did not inhibit nicotine-evoked $^{86}Rb^+$ efflux (Fig. 3).

Inhibition of [^{3}H]MLA Binding. Although completely inhibiting [^{3}H]MLA binding to membranes prepared from whole rat brain, lobeline exhibited low affinity (K_i = 11.6 μM) for α7* nAChRs (Fig. 4) and was ~20-fold less potent than nicotine in this assay. The 10-hydroxy analogs 10*R*-MESP and 10*S*/10*R*-MEPP were ~4- to 8-fold more potent than lobeline in this assay. Lobelanidine was 3-fold more potent than lobeline. Lobeline tosylate, ketoalkene lobelanine, and lobelane had similar affinity to lobeline at the [^{3}H]MLA binding site. MTD and (−)-TTD did not inhibit [^{3}H]MLA binding at the concentrations examined, demonstrating no affinity for α7* nAChRs. Thus, defunctionalization of lobeline decreases affinity for α7* nAChRs.

Inhibition of [^{3}H]DA Uptake. Lobeline and each of the lobeline analogs completely inhibited specific [^{3}H]DA uptake into rat striatal synaptosomes, but with varying affinity (Fig. 5). GBR-12909 inhibited [^{3}H]DA uptake (K_i = 18 nM), consistent with previously reported results (Carroll et al., 2002). Also in agreement with previous reports (Teng et al., 1997), lobeline inhibited (K_i = 29.4 μM) [^{3}H]DA uptake but had low affinity for this site. The highly functionalized analogs lobelanidine (a dihydroxy analog), lobeline tosylate (the *O*-8-tosyl sulfonic acid ester), and lobelanine (a diketo analog) were equipotent (K_i = 16–33 μM) with lobeline in inhibiting [^{3}H]DA uptake. Ketoalkene, lobelane, 10*S*/10*R*-MEPP, and 10*R*-MESP were 5- to 34-fold more potent than lobeline. Although an order of magnitude less potent than GBR-12909, the defunctionalized and unsaturated C-6 epimers MTD and (−)-TTD were the most potent analogs in inhibiting [^{3}H]DA uptake, being 50- to 100-fold more potent in inhibiting DAT compared with lobeline and exhibiting a surprising lack of stereoselectivity. Thus, the removal of the functionalities from the C-2 and C-6 side chains of lobeline and the introduction of unsaturation [MTD and (−)-TTD] afforded the most potent analogs in the [^{3}H]DA uptake assay.

Kinetic Analysis of the Inhibition of [^{3}H]DA Uptake. To determine whether lobeline and selected lobeline analogs inhibited [^{3}H]DA uptake competitively or noncompetitively, kinetic analyses were performed, and the results are illustrated in Fig. 6 and Table 2. Concentrations of lobeline (60 μM), MTD (3 μM), (−)-TTD (1 μM), and lobelane (1 μM) were chosen based on their IC_{50} values obtained from the inhibition curves illustrated in Fig. 5. Lobeline decreased the V_{max} compared with control (t_5 = 3.16, $P < 0.05$) without altering the K_m (t_5 = 0.39, P = 0.72; Fig. 6A, Table 2), indicating that lobeline noncompetitively inhibits [^{3}H]DA uptake into striatal synaptosomes. Similarly, lobelane inhibited [^{3}H]DA uptake in a noncompetitive manner, decreasing the V_{max} (t_5 = 2.57, P = 0.05) without altering the K_m (t_5 = 1.38, P = 0.23; Fig. 6B, Table 2). In contrast to lobeline and lobelane, the defunctionalized unsaturated stereoisomers MTD and (−)-TTD increased the K_m compared with control (t_5 = 4.49, $P <$ 0.05 and t_6 = 6.65, $P < 0.001$, respectively; Fig. 6, C and D, Table 2) without altering the V_{max} (t_5 = 0.28, P = 0.79 and t_6 = 0.33, P = 0.76, respectively), indicating competitive inhibition of DAT.

Inhibition of [^{3}H]5-HT Uptake. Lobeline and its analogs completely inhibited specific [^{3}H]5-HT uptake into rat hippocampal synaptosomes, but with varying affinity (Fig. 7). Consistent with previous reports (Fuller et al., 1991), fluoxetine inhibited specific [^{3}H]5-HT uptake with a K_i of 41 nM. Lobeline and lobelanidine were the least potent analogs, with K_i values of ~25 μM. Lobelanine, lobelane, lobeline tosylate, and ketoalkene were 8- to 16-fold more potent than lobeline in inhibiting [^{3}H]5-HT uptake. (−)-TTD was 24-fold more potent than its C-6 epimer MTD in inhibiting [^{3}H]5-HT uptake, and both epimers were more potent than lobeline in this assay. Both C-10 monohydroxy analogs 10*S*/10*R*-MEPP and 10*R*-MESP had high affinity for SERT (K_i = 10 and 44 nM, respectively), constituting the most potent analogs in the

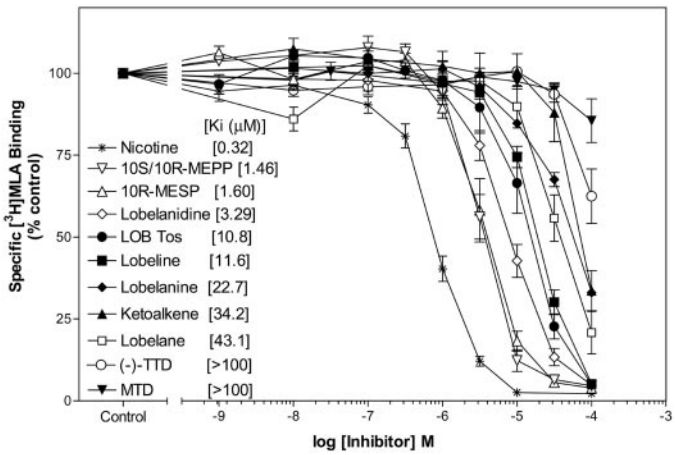

Fig. 4. Lobeline and lobeline analogs inhibit [^{3}H]MLA binding to rat whole brain membranes. Nicotine was used as a standard for comparison. Nonspecific binding was determined in the presence of nicotine (1 mM). K_i values for lobeline and its analogs are provided in brackets. Data are the mean (±S.E.M.) specific binding presented as a percentage of the control condition (mean ± S.E.M., 89.6 ± 2.5 fmol/mg; n = 4 rats per compound).

series. Furthermore, 10*S*/10*R*-MEPP and 10*R*-MESP were equipotent with fluoxetine. Importantly, these monohydroxy analogs were ~2 to 3 orders of magnitude more potent than lobeline.

Inhibition of [^{125}I]RTI-55 Binding and [^{3}H]DA, [^{3}H]5-HT, and [^{3}H]NE Uptake by hDAT, hSERT, and hNET, Respectively, in Stably Expressed HEK-293 Cells. Similar to what has been previously shown for a number of uptake inhibitors (Eshleman et al., 1999), the potency of lobeline and its analogs in inhibiting hDAT and hSERT function ([^{3}H]DA and [^{3}H]5-HT uptake, respectively) was correlated with potency in inhibiting [^{125}I]RTI-55 binding in the cell lines expressing the respective transporters. The relationship between neurotransmitter uptake and binding was less apparent for hNET in both the previous and current studies. In binding and uptake assays, lobeline generally exhibited low affinity for hDAT, hSERT, and hNET compared with cocaine, and, similar to cocaine, lobeline did not exhibit selectivity at these transporter sites (Table 3). In both [^{125}I]RTI-55 binding and [^{3}H]DA uptake assays, the defunctionalized saturated analog lobelane (K_i = 97 and 87 nM, respectively) was ~50-fold more potent than lobeline in inhibiting hDAT. In contrast to lobeline, lobelane demonstrated high nanomolar affinity for hSERT. Whereas lobelane was equipotent to lobeline in the [^{125}I]RTI-55 binding assay probing hNET, lobelane was 33-fold more potent than lobeline in inhibiting [^{3}H]NE uptake via hNET expressed in HEK-293 cells. Furthermore, lobelane showed only a 6- to 10-fold selectivity for hDAT over hSERT. However, lobelane was 18-fold more selective for hDAT compared with hNET in the binding assay but demonstrated no selectivity between hDAT and hNET in the uptake assay. The defunctionalized unsaturated analog MTD was at least 100-fold more potent than lobeline at hDAT and hSERT in both [^{125}I]RTI-55 binding and uptake assays. With respect to hNET, MTD was 7- to 14-fold more potent than lobeline in binding and uptake assays. Generally, the affinity of MTD for these three transporters was not different from that obtained for lobelane in these assays (≤ a 7-fold difference between MTD and lobelane; Table 3). In the [^{125}I]RTI-55 binding assays, MTD was 44-fold more selective for hDAT over hSERT and 7-fold more selective for hDAT over hSERT. Similarly, MTD was 40-fold more selective for hDAT over hSERT in the uptake assays, whereas this analog showed no selectivity for hDAT compared with hNET in the uptake assay. Generally, the Hill coefficients for all of the compounds approximated unity, suggesting competition with [^{125}I]RTI-55 at a single binding site.

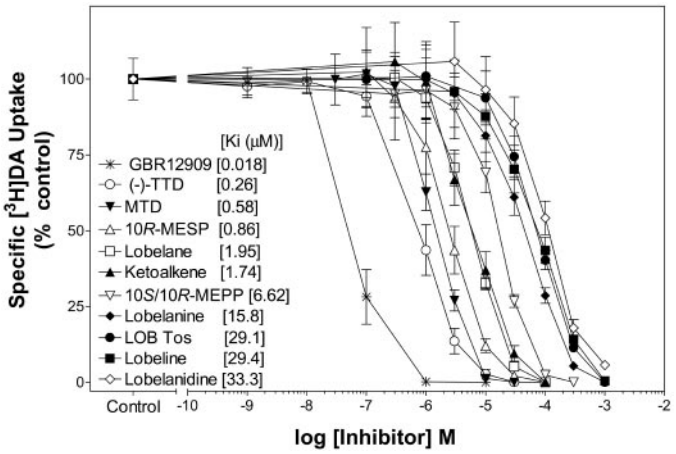

Fig. 5. Lobeline and lobeline analogs inhibit specific [^{3}H]DA uptake into rat striatal synaptosomes. GBR-12909, a specific DAT inhibitor, was used as a standard for comparison. Nonspecific uptake was determined in the presence of nomifensine (10 μM). K_i values for lobeline and its analogs are provided in brackets. Data are the mean (±S.E.M.) specific [^{3}H]DA uptake presented as a percentage of the control condition (mean ± S.E.M., 43.5 ± 1.9 fmol/mg; n = 4–6 rats per compound).

Inhibition of [^{3}H]MTBZ Binding. Lobeline and its analogs inhibited [^{3}H]MTBZ binding to vesicle membranes prepared from rat whole brain (Fig. 8). With the exception of lobelanidine, this series of compounds exhibited a narrow range of K_i values (0.92–8.8 μM). Lobelane was the most potent of the analogs in this series (K_i = 920 nM), and lobelanidine was the least potent (K_i = 26 μM). In contrast to the results obtained for inhibition of [^{3}H]DA and [^{3}H]5-HT uptake in rat brain synaptosomes, lobeline and its analogs were equipotent in inhibiting [^{3}H]MTBZ binding to vesicle membranes, with the exception of ketoalkene and lobelane, which were both more potent at VMAT2 than lobeline. Furthermore, MTD was significantly more potent than its epimer (−)-TTD in inhibiting [^{3}H]MTBZ binding to vesicle membranes.

Discussion

The current SAR analysis investigated effects of defunctionalized, esterified, reduced, and oxidized lobeline analogs on α4β2* and α7* nAChRs and monoamine plasmalemma and vesicular monoamine transporters. As previously reported, lobeline has high affinity for [^{3}H]nicotine binding sites in rodent striatal membrane preparations (K_i = 4–20 nM) (Abood et al., 1988; Reavill et al., 1990; Bhat et al., 1991; Court et al., 1994; Flammia et al., 1999). Defunctionalized lobeline analogs lobelane, MTD, and (−)-TTD generally exhibited decreased affinity for [^{3}H]nicotine binding sites (α4β2* nAChRs). MTD, an unsaturated, *cis*-defunctionalized analog of lobeline, did not interact with α4β2* sites; however, its C-6 epimer (−)-TTD showed enhanced interaction with

the $\alpha4\beta2*$ site, indicating that stereochemical factors play a role in binding site recognition. However, the affinity of (−)-TTD for the [^{3}H]nicotine binding site was 3 orders of magnitude less than that of lobeline. Partially defunctionalized analogs ketoalkene and 10*S*/10*R*-MEPP exhibited intermediate affinity for $\alpha4\beta2*$ nAChRs, with 30-fold lower affinity than lobeline. Structurally related analogs lobelanine and lobelanidine had 2 to 3 orders of magnitude lower affinity than lobeline in the [^{3}H]nicotine binding assay, consistent with results from previous studies (Flammia et al., 1999). Lobeline and lobeline tosylate were equipotent in the [^{3}H]nicotine binding assay, which assesses interaction with high-affinity $\alpha4\beta2*$ nAChRs. The latter results suggest that increases in molecular volume and steric bulk adjacent to the 8-hydroxy group by the addition of the tosyl sulfonate moiety can be accommodated at the high-affinity $\alpha4\beta2*$ site. Although a correlation between inhibition of [^{3}H]nicotine binding and inhibition of nicotine-evoked $^{86}Rb^+$ efflux was expected, tosylation of the 8-hydroxy group surprisingly provided an analog (lobeline tosylate) with higher potency than lobeline in the $^{86}Rb^+$ efflux assay. This lack of correlation may be the result of different modes of interaction of these compounds at the high-affinity $\alpha4\beta2*$ nAChRs (e.g., competitive versus noncompetitive).

The $^{86}Rb^+$ efflux assay assesses functional response at $\alpha4\beta2*$ nAChRs (Marks et al., 1995; Miller et al., 2000). Effects of fully and partially defunctionalized analogs were evaluated in this assay to ascertain whether these analogs act as nAChR agonists or antagonists. Neither lobeline nor its analogs evoked $^{86}Rb^+$ efflux, demonstrating that these compounds are not agonists at $\alpha4\beta2*$ nAChRs. Lobeline acts as an $\alpha4\beta2*$ nAChR antagonist (Miller et al., 2000), and the current findings are consistent with these previous results. Ketoalkene and lobeline tosylate both inhibited [^{3}H]nicotine binding to striatal membranes and inhibited nicotine-evoked $^{86}Rb^+$ efflux from thalamic synaptosomes, demonstrating antagonism of $\alpha4\beta2*$ nAChRs. MTD, which did not inhibit [^{3}H]nicotine binding, also did not inhibit nicotine-evoked $^{86}Rb^+$ efflux, indicating that it does not interact with $\alpha4\beta2*$ sites either competitively or noncompetitively.

In general, the members of this series of lobeline analogs have low affinity for $\alpha7*$ nAChRs. The C-10 hydroxy analogs 10*S*/10*R*-MEPP and 10*R*-MESP were the most potent in the series but were 5-fold less potent than nicotine. Because lobeline is progressively defunctionalized, affinity for $\alpha7*$ nAChRs is decreased, and selectivity between $\alpha4\beta2*$ and $\alpha7*$ is diminished or eliminated, mainly due to the marked decrease in affinity for $\alpha4\beta2*$ nAChRs. Conversely, lobeline and

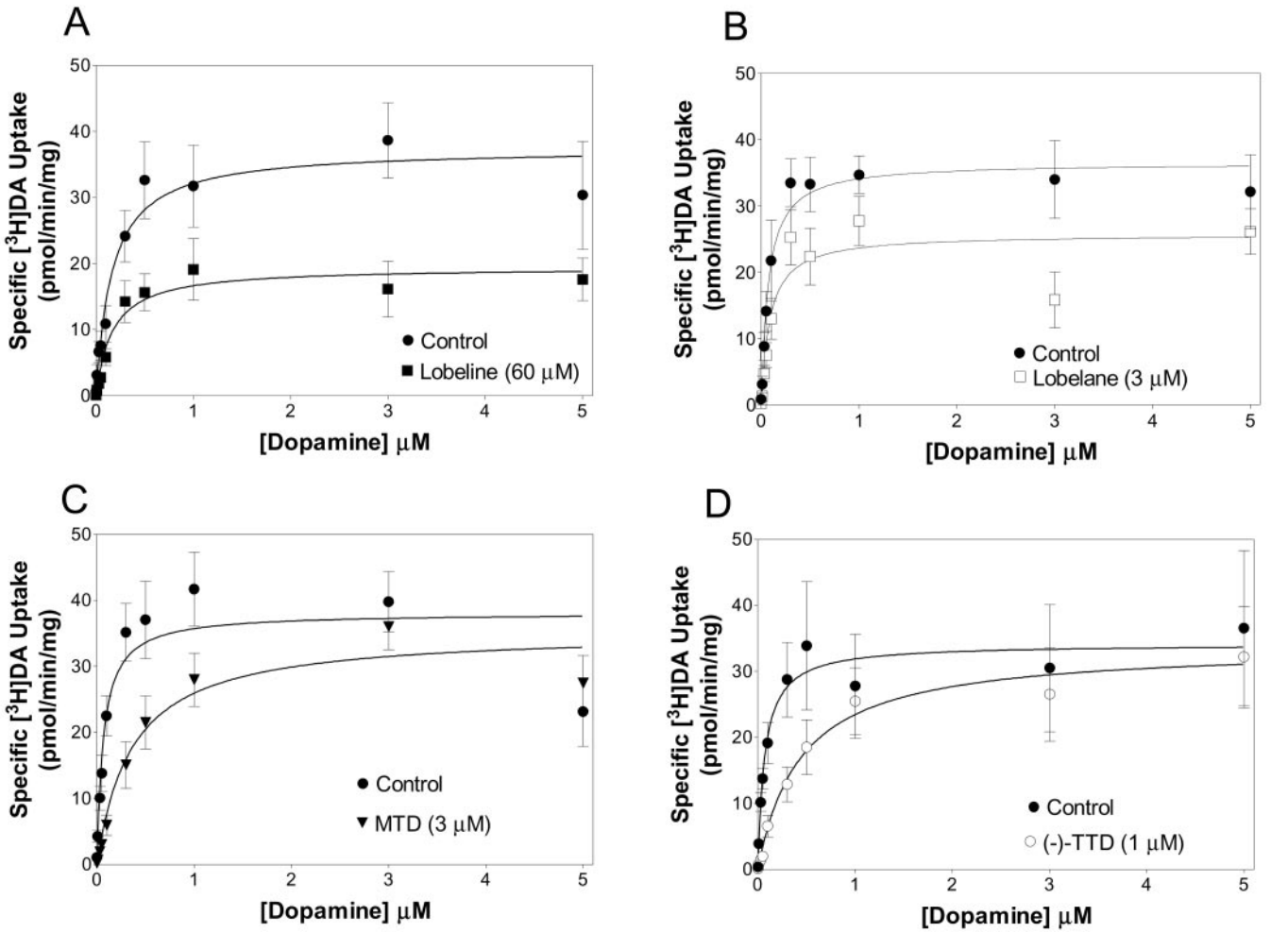

Fig. 6. Kinetic analysis of the inhibition of specific [^{3}H]DA uptake by lobeline, lobelane, MTD, and (−)-TTD. Concentrations of lobeline (60 μM; panel A), lobelane (3 μM; panel B), MTD (1 μM; panel C) and (−)-TTD (3 μM; panel D) were chosen from the concentration-response curves illustrated in Fig. 5. Nonspecific uptake was determined in the presence of nomifensine (10 μM). K_m and V_{max} values are presented in Table 2 (n = 6–7 rats per compound).

TABLE 2

Lobeline (60 μM) and lobelane (3 μM) inhibit DAT function via a noncompetitive mechanism, whereas MTD (3 μM) and (−)-TTD (1 μM) competitively inhibit DAT function in rat striatal synaptosomes

Data are presented as mean ± S.E.M. values for K_m and V_{max}. Nonspecific [^{3}H]DA uptake was determined in the presence of nomifensine (10 μM). No significant differences were found in V_{max} or K_m values between control groups (parameters determined in the absence of drug) in the four series of experiments. Control values for specific [^{3}H]DA uptake were combined for tabular presentation. Concentration-response curves are presented in Fig. 6.

Compound	K_m	V_{max}
	μM	*pmol/min/mg*
Control	0.270 ± 0.138[a]	35.7 ± 5.75
Lobeline	0.312 ± 0.145	19.0 ± 3.95*
Lobelane	0.135 ± 0.078	26.8 ± 4.74*
MTD	0.507 ± 0.126*	33.0 ± 12.5
(−)-TTD	0.398 ± 0.161*	37.0 ± 3.78

[a] Values are presented as mean (±S.E.M.) K_m or V_{max} values; n = 6 to 7 rats per group.

*$P < 0.05$ different from control.

lobeline tosylate are nearly 3 orders of magnitude more selective for $\alpha4\beta2*$ nAChRs than $\alpha7*$ nAChRs.

Lobeline interacts nonselectively with monoamine transporters (DAT, SERT, NET, and VMAT2), consistent with previous findings (Teng et al., 1997, 1998; Dwoskin and Crooks, 2002). Lobeline exhibited the highest affinity, albeit in the low micromolar range, for VMAT2. Generally, defunctionalization of the lobeline molecule provided analogs with higher affinity for the plasmalemma transporters. Specifically, two compounds, MTD and (−)-TTD, were 1 to 2 orders of magnitude more potent than lobeline in inhibiting DAT function. Lobelane (a defunctionalized, fully saturated analog) and 10*R*-MESP and ketoalkene (partially defunctionalized analogs) were 15- to 30-fold more potent than lobeline in inhibiting DAT function. Both lobeline and lobelane inhibited DAT function noncompetitively. Interestingly, the unsaturated, defunctionalized epimers MTD and (−)-TTD competitively inhibited DAT. Taken together, it seems that this series of analogs interact with at least two different sites on DAT. The more rigid unsaturated epimers MTD and (−)-TTD compete with the substrate site, whereas the flexible, fully saturated analog lobelane seems to interact with an alternative site on DAT.

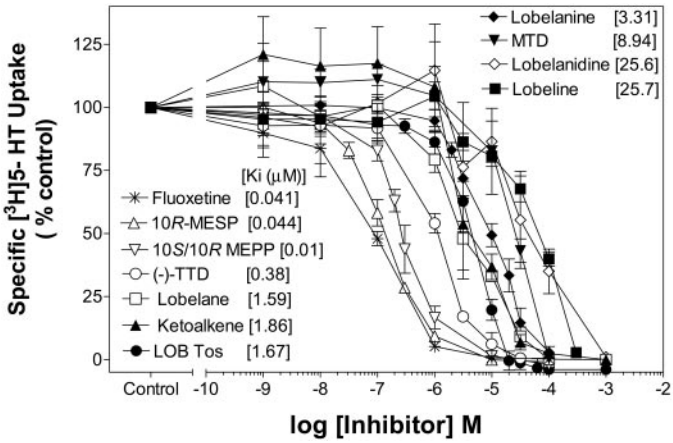

Fig. 7. Lobeline and lobeline analogs inhibit specific [^{3}H]5-HT uptake into rat hippocampal synaptosomes. Fluoxetine, a specific SERT inhibitor, was used as a standard for comparison. Nonspecific uptake was determined in the presence of fluoxetine (10 μM). K_i values are provided in brackets. Data are the mean (±S.E.M.) specific [^{3}H]5-HT uptake presented as a percentage of the control condition (mean ± S.E.M., 1.39 ± 0.08 pmol/min/mg; n = 4–6 rats per compound).

With respect to inhibition of SERT, (−)-TTD was 24-fold more potent than its C-6 epimer MTD, indicating that SERT is sensitive to the stereochemistry at C-6, whereas DAT and VMAT2 are not. Partially defunctionalized analogs 10*S*/10*R*-MEPP and 10*R*-MESP were 2 to 3 orders of magnitude more potent than lobeline in inhibiting SERT function. These analogs had affinity similar to fluoxetine, a drug that selectively inhibits SERT (Fuller et al., 1991). Defunctionalization of lobeline at C-8 and the introduction of a C-10 hydroxy group affords 10*S*/10*R*-MEPP and 10*R*-MESP, both of which exhibit high affinity for SERT. The removal of the C-10 hydroxy group from 10*S*/10*R*-MEPP and 10*R*-MESP afforded lobelane and MTD, respectively, both of which exhibited an ~200-fold lower affinity at SERT. Thus, the completely defunctionalized analogs (lobelane and MTD) have low affinity for and little or no selectivity between DAT and SERT. Moreover, 10*S*/10*R*-MEPP showed 600-fold more selectivity in inhibiting SERT over DAT. Therefore, the C-10 hydroxy group seems to be a critical functionality for selective interaction with SERT. Taken together, the results suggest that 10*S*/10*R*-MEPP may be a potential lead compound for the development of new therapeutic agents for the treatment of mood disorders.

Lobeline, lobelane, and MTD were investigated for their interaction with DAT, SERT, and NET expressed in HEK-293 cells to further investigate their selectivity for specific transporters. Consistent with previous findings (Eshleman et al., 1999), the current study generally shows similar results (i.e., the same rank order of transporter inhibition for the compounds) in the hDAT and hSERT expression systems compared with rat DAT and SERT in brain synaptosomal preparations. By and large, higher affinity for these analogs was observed in the expression systems than in native tissues, but this may be a consequence of comparison between human and rat transporters. In contrast, more variable results comparing binding and uptake assays using cell expression systems were obtained with respect to NET. Interaction of lobeline, lobelane, and MTD with NET was not determined in rat brain; however, results from HEK-293 cells suggest that lobelane and MTD should inhibit [^{3}H]NE uptake in brain more potently than lobeline.

Lobelane and ketoalkene were significantly more potent than lobeline in inhibiting binding of [^{3}H]MTBZ to VMAT2 in whole brain synaptic vesicle preparations. Although there was only a 5-fold difference in affinity between K_i values for lobeline and these two analogs, the confidence intervals for lobelane and ketoalkene did not overlap with that for lobeline, indicating significant differences in affinity for VMAT2. Similarly, MTD exhibited a significantly higher affinity for VMAT2 compared with (−)-TTD, although only a 4-fold difference in affinity was observed. These results indicate a modest enhancement of affinity at VMAT2 for these analogs over lobeline. The SAR trends for VMAT2 interaction indicate that the introduction of a 10*R* hydroxy group into the lobeline molecule reduces affinity for VMAT2, and complete defunctionalization of the lobeline molecule affords analogs with the highest affinity for VMAT2 in the series.

The series of lobeline analogs assessed in the current study were generally more potent than lobeline at DAT, SERT, NET, and VMAT2, demonstrating that appropriate modifi-

TABLE 3
Lobeline, lobelane, and MTD inhibit [^{125}I]RTI-55 binding and [^{3}H]neurotransmitter uptake into recombinant hDAT, hSERT, and hNET stably expressed in HEK-293 cells

Compound	[^{125}I]RTI-55 Binding K_i	Hill Coefficient	[^{3}H]Neurotransmitter Uptake IC_{50}
	μM		μM
HEK-hDAT cells			
Lobeline	5.40 ± 1.30[a]	−1.03 ± 0.10	>10
Lobelane	0.097 ± 0.033	−0.92 ± 0.06	0.087 ± 14
MTD	0.043 ± 0.015	−0.80 ± 0.07	0.117 ± 0.033
Cocaine	0.469 ± 0.037	−1.19 ± 0.12	0.524 ± 0.055
HEK-hSERT cells			
Lobeline	>10		ND
Lobelane	0.530 ± 0.130	−0.930	0.830 ± 0.320
MTD	1.89 ± 0.29	−0.99 ± 0.09	4.80 ± 1.20
Cocaine	0.353 ± 0.030	−1.07 ± 0.03	0.419 ± 0.037
HEK-hNET cells			
Lobeline	1.87 ± 0.82	−0.58 ± 0.05	2.79 ± 0.480
Lobelane	1.80 ± 0.47	−0.97 ± 0.14	0.085 ± 0.006
MTD	0.277 ± 0.082	−0.79 ± 0.04	0.198 ± 0.070
Cocaine	2.42 ± 0.12	−0.87 ± 0.04	0.370 ± 0.056

ND, not determined.
[a] Values are presented as means (±S.E.M.) from at least three independent experiments. Each experiment was conducted in duplicate (binding) or triplicate (uptake).

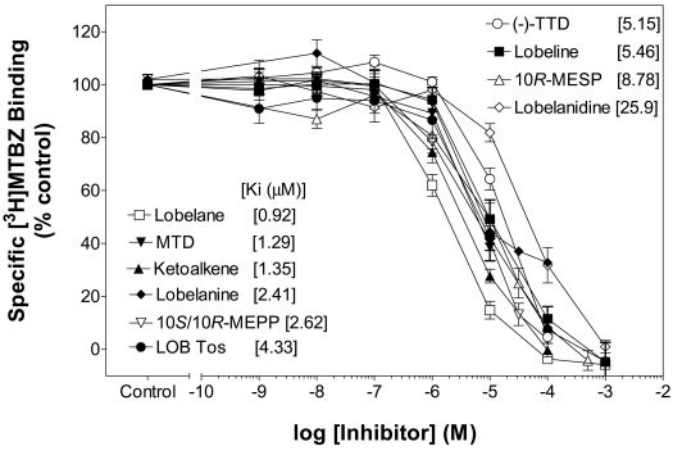

Fig. 8. Lobeline and lobeline analogs inhibit specific [^{3}H]MTBZ binding to vesicles prepared from rat whole brain. Nonspecific binding was determined in the presence of tetrabenazine (20 μM). K_i values are reported in brackets. Data are the mean (±S.E.M.) specific [^{3}H]MTBZ binding presented as a percentage of the control condition (mean ± S.E.M., 226 ± 10.8 fmol/mg; n = 4–6 rats per compound).

cation of lobeline affords compounds with higher affinity at these sites. These transporters have been implicated in the behavioral activation induced by methamphetamine and cocaine (e.g., Kuhar et al., 1991; Sulzer et al., 1995; Johnson et al., 1998; Brown et al., 2000, 2001). Comparison across transporter assays provides an indication of the selectivity exhibited by these analogs. Lobeline was significantly more potent at VMAT2 than at plasmalemma transporters, although only a 5-fold difference in selectivity was observed. The structurally related *Lobelia* alkaloid lobelanidine showed no selectivity at these transporter sites, whereas lobelanine, another *Lobelia* alkaloid, exhibited a 5- to 7-fold selectivity for SERT and VMAT2 over DAT. Lobeline tosylate was 6- to 17-fold more selective for SERT over DAT and VMAT2; however, affinity of this compound for SERT was in the low micromolar range. Although lobelane and ketoalkene were among the most potent inhibitors at VMAT2, these analogs showed no selectivity between transporters. (−)-TTD showed significantly greater (14–20-fold) selectivity for the plasmalemma transporters over VMAT2, whereas its C-6 epimer MTD showed greater selectivity for DAT over SERT but was not selective with regard to DAT and VMAT2. 10*R*-MESP, which exhibited high affinity at SERT (K_i = 44 nM), showed a 20-fold selectivity at SERT over DAT and a 200-fold selectivity at SERT over VMAT2. The epimeric mixture 10*S*/10*R*-MEPP exhibited the highest affinity (K_i = 10 nM) at SERT and was 660-fold more selective for SERT than for DAT and 260-fold more selective for SERT than for VMAT2. Thus, since 10*S*/10*R*-MEPP demonstrated good selectivity at SERT and was devoid of nAChR activity, selectivity between plasmalemma transporters can be achieved through structural modification of the lobeline molecule.

Findings from this initial SAR study demonstrate that defunctionalization of lobeline markedly decreases affinity for $\alpha4\beta2*$ and $\alpha7*$ nAChRs while increasing affinity and selectivity for monoamine neurotransmitter transporters. These results suggest that the oxygen functionalities in the lobeline molecule are critical for interaction with nAChRs but not for interaction with neurotransmitter transporters. Monoamine transporters are considered valid targets for drug development for the treatment of methamphetamine abuse. In this respect, little is known regarding the VMAT2 pharmacophore. Drug discovery targeting VMAT2 may provide a unique opportunity to probe the underlying neurochemical mechanisms responsible for psychostimulant abuse and yield novel approaches for treatment. Subsequent SAR studies will be directed at enhancing selectivity of lobeline analogs for individual transporters.

Acknowledgments

We acknowledge the technical assistance of M. Dathan Chesnut, David Eaves, Gabriela Deaciuc, and Anne Woods. We also acknowledge Dr. Michael Kilbourn, who generously supplied [^{3}H]MTBZ [supported by National Institutes of Health (NIH) Grant MH 47611].

References

Abood LG, Shahid K, and Maiti A (1988) Structure-activity studies of carbamate and other esters: agonists and antagonists to nicotine. *Pharmacol Biochem Behav* **30:**403–408.
Bhat RV, Marks MJ, and Collins AC (1991) Effects of chronic nicotine infusions on kinetics of high-affinity nicotine binding. *J Neurochem* **62:**574–581.
Bradford MM (1976) A rapid and sensitive method for the quantitation of microgram quantities of protein utilizing the principle of protein-dye binding. *Anal Biochem* **72:**248–253.
Brown JM, Hanson GR, and Fleckenstein AE (2000) Methamphetamine rapidly decreases vesicular dopamine uptake. *J Neurochem* **74:**2221–2223.
Brown JM, Hanson GR, and Fleckenstein AE (2001) Regulation of the vesicular

monoamine transporter-2: a novel mechanism for cocaine and other psychostimulants. *J Pharmacol Exp Ther* **296:**762–767.
Carroll FI, Lewin AH, and Marscarella SW (2002) Dopamine-transporter uptake blockers: structure-activity relationships, in *Neurotransmitter Transporters: Structure, Function and Regulation* (Reith ME ed) pp 381–432, Humana Press, Totowa, NJ.
Cheng YC and Prusoff WH (1973) Relationship between the inhibition constant (K_I) and the concentration of inhibitor which causes 50 percent inhibition (I_{50}) of an enzymatic reaction. *Biochem Pharmacol* **22:**3099–3108.
Court JA, Perry EK, Spurden D, Lloyd S, Gillespie JI, Whiting P, and Barlow R (1994) Comparison of the binding of nicotinic agonists to receptors from human and rat cerebral cortex and from chick brain ($\alpha4\beta2$) transfected into mouse fibroblasts with ion channel activity. *Brain Res* **667:**118–122.
Crooks PA, Ravard A, Wilkins LH, Teng LH, Buxton ST, and Dwoskin LP (1995) Inhibition of nicotine-evoked [^{3}H]dopamine release by pyridino N-substituted nicotine analogues: a new class of nicotinic antagonist. *Drug Dev Res* **36:**91–102.
Dwoskin LP and Crooks PA (2002) A novel mechanism and potential use for lobeline as a treatment for psychostimulant abuse. *Biochem Pharmacol* **63:**89–98.
Eshleman AJ, Carmolli M, Cumbay M, Martens CR, Neve KA, and Janowsky A (1999) Characteristics of drug interactions with recombinant biogenic amine transporters expressed in the same cell type. *J Pharmacol Exp Ther* **289:**877–885.
Flammia D, Malgorzata D, Damaj MI, Martin B, and Glennon RA (1999) Lobeline: structure-affinity investigation of nicotinic acetylcholinergic receptor binding. *J Med Chem* **42:**3726–3731.
Fuller RW, Wong DT, and Robertson DW (1991) Fluoxetine, a selective inhibitor of serotonin uptake. *Med Res Rev* **11:**17–34.
Green TA, Miller DK, Wong MY, Harrod SB, Crooks PA, Bardo MT, and Dwoskin LP (2001) Lobeline attenuates methamphetamine and cocaine self-administration and locomotor sensitization in rats. *Soc Neurosci Abstr* 878.1.
Harrod SB, Dwoskin LP, Crooks PA, Klebaur JE, and Bardo MT (2001) Lobeline attenuates *d*-methamphetamine self-administration in rats. *J Pharmacol Exp Ther* **298:**172–179.
Harrod SB, Dwoskin LP, Green TA, Gehrke BJ, and Bardo MT (2003) Lobeline does not serve as a reinforcer in rats. *Psychopharmacology* **165:**397–404.
Johnson RA, Eshleman AJ, Meyers T, Neve KA, and Janowsky A (1998) [^{3}H]Substrate- and cell-specific effects of uptake inhibitors on human dopamine and serotonin transporter-mediated efflux. *Synapse* **30:**97–106.
Kenakin T (1997) *Pharmacologic Analysis of Drug-Receptor Interaction.* Lippincott-Raven, Philadelphia.
Koob GF (1992) Neural mechanisms of drug reinforcement. *Ann NY Acad Sci* **654:**171–191.
Kuhar MJ, Ritz MC, and Boja JW (1991) The dopamine hypothesis of the reinforcing properties of cocaine. *Trends Neurosci* **14:**299–302.
Lendvai B, Sershen H, Lajtha A, Santha E, Baranyi M, and Vizi ES (1996) Differential mechanisms involved in the effect of nicotinic agonists DMPP and lobeline to release [^{3}H]5-HT from rat hippocampal slices. *Neuropharmacology* **35:**1769–1777.
Lukas RJ, Changeux JP, Le Novere N, Albuquerque EX, Balfour DJ, Berg DK, Bertrand D, Chiappinelli VA, Clarke PB, Collins AC, et al. (1999) International Union of Pharmacology. XX. Current status of the nomenclature for nicotinic acetylcholine receptors and their subunits. *Pharmacol Rev* **51:**397–401.
Marks MJ, Bullock AK, and Collins AC (1995) Sodium channel blockers partially inhibit nicotine-stimulated $^{86}Rb^+$ efflux from mouse brain synaptosomes. *J Pharmacol Exp Ther* **274:**1–9.
Marks MJ, Farnham DA, Grady SR, and Collins AC (1993) Nicotinic receptor function determined by stimulation of rubidium efflux from mouse brain synaptosomes. *J Pharmacol Exp Ther* **264:**542–552.
Marks MJ, Whiteaker P, Calcaterra J, Stitzel JA, Bullock AE, Grady SR, Picciotto MR, Changeux JP, and Collins AC (1999) Two pharmacologically distinct components of nicotinic receptor-mediated rubidium efflux in mouse brain require the beta2 subunit. *J Pharmacol Exp Ther* **289:**1090–1103.
Miller DK, Crooks PA, and Dwoskin LP (2000) Lobeline inhibits nicotine-evoked [^{3}H]dopamine overflow from rat striatal slices and nicotine-evoked $^{86}Rb^+$ efflux from thalamic synaptosomes. *Neuropharmacology* **39:**2654–2662.
Miller DK, Crooks PA, Teng L, Witkin JM, Munzar P, Goldberg SR, Acri JB, and Dwoskin LP (2001) Lobeline inhibits the neurochemical and behavioral effects of amphetamine. *J Pharmacol Exp Ther* **296:**1023–1034.
Miller DK, Harrod SB, Green TA, Wong MY, Bardo MT, and Dwoskin LP (2002) Lobeline attenuates the locomotor stimulation induced by repeated nicotine administration in rats. *Pharmacol Biochem Behav* **74:**279–286.
Reavill C, Walther B, Stolerman IP, and Testa B (1990) Behavioral and pharmacokinetics studies on nicotine, cytisine and lobeline. *Neuropharmacology* **36:**619–624.
Rocha BA, Fumagalli F, Gainetdinov RR, Jones SR, Ator R, Giros B, Miller GW, and Caron MG (1998) Cocaine self-administration in dopamine transporter knockout mice. *Nat Neurosci* **1:**132–137.
Sharples CG, Kaiser S, Soliakov L, Marks MJ, Collins AC, Washburn M, Wright E, Spenser JA, Gallagher T, Whiteaker P, et al. (2000) UB-165: a novel nicotinic agonist with subtype selectivity implicates the alpha4beta2* subtype in the modulation of dopamine release from rat striatal synaptosomes. *J Neurochem* **20:**2783–2791.
Sora I, Wichems C, Takahashi N, Li XF, Zeng Z, Revay R, Lesch KP, Murphy DL, and Uhl GR (1998) Cocaine reward models: conditioned place preference can be established in dopamine- and in serotonin-transporter knock out mice. *Proc Natl Acad Sci USA* **95:**7699–7704.
Sulzer D, Chen TK, Lau YY, Kristensen H, Rayport S, and Ewing A (1995) Amphetamine redistributes dopamine from synaptic vesicles to the cytosol and promotes reverse transport. *J Neurosci* **15:**4102–4108.
Takahashi N, Miner LL, Sora I, Ujike H, Revay RS, Kostic V, Jackson-Lewis V, Prezedborski S, and Uhl GR (1997) VMAT2 knockout mice: heterozygotes display reduced amphetamine conditioned reward, enhanced amphetamine locomotion and enhanced MPTP toxicity. *Proc Natl Acad Sci USA* **94:**9938–9943.
Taylor P and Insel PA (1990) Molecular basis of pharmacologic selectivity, in *Principles of Drug Action* (Pratt WB and Taylor P eds) pp 1–102, Churchill Livingstone, Philadelphia.
Teng L, Crooks PA, and Dwoskin LP (1998) Lobeline displaces [^{3}H]dihydroxytetrabenazine binding and releases [^{3}H]dopamine from rat striatal synaptic vesicles: comparison with *d*-amphetamine. *J Neurochem* **71:**258–265.
Teng L, Crooks PA, Sonsalla PK, and Dwoskin LP (1997) Lobeline and nicotine evoke [^{3}H]overflow from rat striatal slices preloaded with [^{3}H]dopamine: differential inhibition of synaptosomal and vesicular [^{3}H]dopamine uptake. *J Pharmacol Exp Ther* **280:**1432–1444.
Wise RA and Bozarth MA (1987) A psychomotor stimulant theory of addiction. *Psychol Rev* **94:**469–492.

Address correspondence to: Dr. Linda P. Dwoskin, College of Pharmacy, University of Kentucky, Lexington, KY, 40536-0082. E-mail: ldwoskin@uky.edu